SHAPE OPTIMIZATION THROUGH PROPER ORTHOGONAL DECOMPOSITION WITH INTERPOLATION AND DYNAMIC MODE DECOMPOSITION ENHANCED BY ACTIVE SUBSPACES

MARCO TEZZELE*, NICOLA DEMO* AND GIANLUIGI ROZZA*

*Mathematics Area, mathLab, SISSA, International School of Advanced Studies,
via Bonomea 265, I-34136 Trieste, Italy
e-mail: marco.tezzele@sissa.it, nicola.demo@sissa.it, gianluigi.rozza@sissa.it

Key words: Nonintrusive Model Order Reduction, Active Subspaces, Free Form Deformation, POD with Interpolation, Dynamic Mode Decomposition, Parameter Space Reduction

Abstract. We propose a numerical pipeline for shape optimization in naval engineering involving two different non-intrusive reduced order method (ROM) techniques. Such methods are proper orthogonal decomposition with interpolation (PODI) and dynamic mode decomposition (DMD). The ROM proposed will be enhanced by active subspaces (AS) as a pre-processing tool that reduce the parameter space dimension and suggest better sampling of the input space.

We will focus on geometrical parameters describing the perturbation of a reference bulbous bow through the free form deformation (FFD) technique. The ROM are based on a finite volume method (FV) to simulate the multi-phase incompressible flow around the deformed hulls.

In previous works we studied the reduction of the parameter space in naval engineering through AS [38, 10] focusing on different parts of the hull. PODI and DMD have been employed for the study of fast and reliable shape optimization cycles on a bulbous bow in [9].

The novelty of this work is the simultaneous reduction of both the input parameter space and the output fields of interest. In particular AS will be trained computing the total drag resistance of a hull advancing in calm water and its gradients with respect to the input parameters. DMD will improve the performance of each simulation of the campaign using only few snapshots of the solution fields in order to predict the regime state of the system. Finally PODI will interpolate the coefficients of the POD decomposition of the output fields for a fast approximation of all the fields at new untried parameters given by the optimization algorithm. This will result in a non-intrusive data-driven numerical optimization pipeline completely independent with respect to the full order solver used and it can be easily incorporated into existing numerical pipelines, from the reference CAD to the optimal shape.

1 Introduction

In a shape optimization problem, we aim to find the shape — among all the admissible geometries — that minimizes a certain objective function. In this work we propose a novel approach to optimize the total resistance of a ship hull advancing in calm water by deforming the original hull, a common problem in the naval engineering field.

First we define the total resistance as the sum of the viscous and lift forces acting on the hull. Formally, our optimization problem can be expressed as

$$\min_{\forall \boldsymbol{\mu} \in D} f(\Omega, \boldsymbol{\mu}) = \min_{\forall \boldsymbol{\mu} \in D} \oint p \cos\theta \, \mathrm{d}\Omega_{\boldsymbol{\mu}} + \oint \tau_x \, \mathrm{d}\Omega_{\boldsymbol{\mu}}, \tag{1}$$

where the $D \subset \mathbb{R}^P$ is the parametric domain, P the number of parameters, $\Omega \in \mathbb{R}^3$ is the reference hull domain, and $\Omega_{\boldsymbol{\mu}} = \mathcal{M}(\Omega, \boldsymbol{\mu})$ is the defomed hull. The morphing map $\mathcal{M}(\cdot, \boldsymbol{\mu}) : \mathbb{R}^3 \to \mathbb{R}^3$ we use in this work is the free form deformation (FFD) and will be properly defined in Section 2. Examples of other deformation techniques are radial basis functions (RBF) interpolation [5, 22, 21], and inverse distance weighting (IDW) interpolation [32, 13, 2]. The unknowns p and τ_x denote respectively the pressure and the x component of the wall shear stress over the hull surface, while θ is the angle between the flow direction and the surface. The evaluation of the objective function requires a numerical simulation of the flow around the ship, which has a high computational cost. The purpose of this work is beyond an analysis of the adopted full order model for the fluid dynamics, we just provide a brief summary in order to facilitate the understanding of the pipeline. We resolve the Reynolds-averaged Navier Stokes (RANS) equations with the k–ω SST turbulence model using a finite volume approach, a typical benchmark in industrial hydrodynamics analysis. Such model deals very well with turbulent fluid, but at high computational cost. Moreover, due to the complexity of the optimization problem, we typically need many evaluations of the objective function to converge to the optimal shape.

For this work we choose to simulate the flow around the DTMB 5415 hull due to the existence of a vast amount of literature and benchmark tests. In Figure 1 the undeformed hull domain.

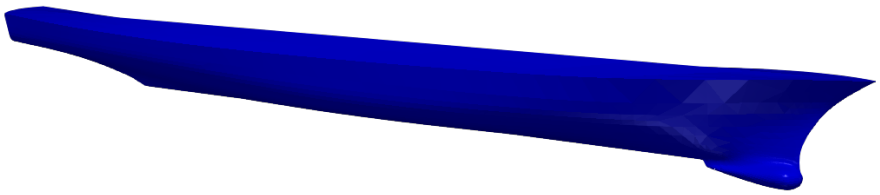

Figure 1: Complete hull domain of the DTMB 5415.

In order to reduce the computational cost, we introduce in the optimization framework two reduced order modeling (ROM) techniques. These techniqes are able to represent complex systems in a low dimensional space, reducing the number of degrees of freedom used in the full order model discretization and providing an efficient and reliable approximation of the solution. The ROM methods initially collect a database of high-fidelity solutions — the solutions

computed using the full-order model — during the most computationally expensive phase, also called *offline* phase. Then, the solutions are combined to build the reduced space we query during the *online* phase to obtain the new solution. In this work, we adopt the dynamic mode decomposition (DMD) and proper orthogonal decomposition with interpolation (PODI), two emerging data-driven techniques. PODI is used to approximate, given the high-fidelity solutions computed for some defomed hulls, the solution for any new parametric point in the domain D. DMD algorithm instead provides a simplification of the dynamics of complex system: we use it in order to accelerate the single high-fidelity simulations we need for PODI method, by storing few system outputs and exploiting them to approximate the flow dynamics. For more details about equation-free ROM methods, we suggest [37], while for a complete overview — including intrusive approaches — we cite [27, 26, 24].

Moreover, additionally to these methods, we use the active subspace (AS) property as pre-processing tool in order to be able to reduce the dimension of the parameter space and obtain a better accuracy in ROM solution approximation.

In this contribution, we focus on all the components of the computational pipeline: in Section 2 we provide a brief overview of the FFD method, the Section 3 illustrates the DMD algorithm, in Section 4 the AS property is explained, while Section 5 describes the idea behind PODI technique. Finally, Sections 6 and 7 provide respectively the numerical results collected during this work and the final conclusions.

2 The free form deformation technique

Free form deformationi (FFD) is a widespread deformation technique. Proposed in [31], FFD was initially employed in computer graphics, getting more popular both in academia and industry in the last decades. In this section, we provide an overview of the method: for more details about FFD, among all the works in literature, we recommend [25, 9, 14].

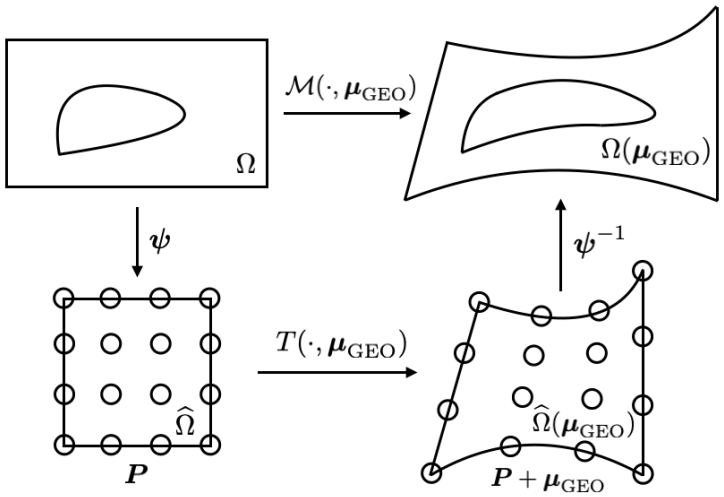

Figure 2: Graphical representation of the FFD morphing map $\mathcal{M}$ as composition of the maps ψ, T, and ψ^{-1}. The displacements of the control points $\boldsymbol{P}$ define the morphing of the domain.

The idea of FFD is very intuitive: the domain is deformed by manipulating a lattice of points surrounding the object to morph. The displacements of these control points are the input parameters $\boldsymbol{\mu}_{\text{GEO}}$. To achieve this result 1) the physical domain Ω is mapped to the reference domain $\widehat{\Omega}$ using the function ψ, and a lattice of control points $\boldsymbol{P}$ is constructed around the object to deform, then 2) through the map T the reference domain is morphed using B-splines or Bernstein polynomials tensor product and finally 3) the deformed domain is remapped to the physical one by using ψ^{-1}. In Figure 2 is shown a sketch of the free form deformation map as a composition of the three functions presented above. Formally, we can define the deformation map $\mathcal{M}$ as

$$\mathcal{M}(\boldsymbol{x}, \boldsymbol{\mu}_{\text{GEO}}) := (\boldsymbol{\psi}^{-1} \circ T \circ \boldsymbol{\psi})(\boldsymbol{x}, \boldsymbol{\mu}_{\text{GEO}}) \quad \forall \boldsymbol{x} \in \Omega. \tag{2}$$

This technique allows to manipulate complex geometries and also computational grids, since it is able to preserve derivatives continuity and perform global deformation using only few parameters. Figure 3 shows the position of the lattice of control points around a bulbous bow, which is the part of the hull we want to parametrize and morph. Regarding the implementation, the results in this contribution are obtained using PyGeM [1], an open source Python package implementing several deformation techniques.

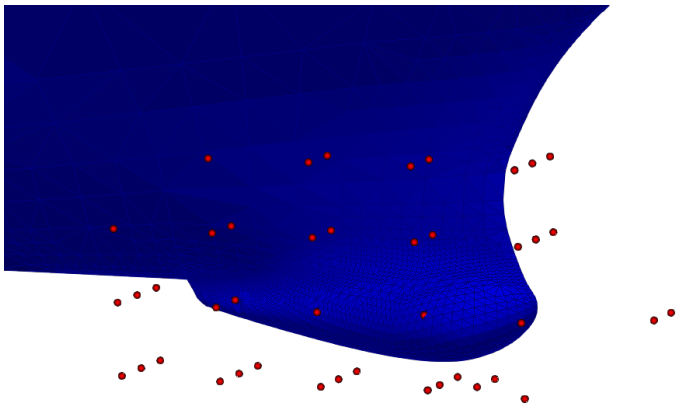

Figure 3: Example of bulbous bow deformation using the FFD method. The red dots are the FFD control points, already manipulated.

3 Dynamic mode decomposition as accelerator of the single simulations

Dynamic mode decomposition is a data-driven modal decomposition technique for analysing the dynamics of nonlinear systems [29, 30]. A comprehensive overview on DMD and its major variants is in [17]. Other nonintrusive approaches with randomized DMD can be found in [4, 3], while naval engineering applications are in [9, 10].

Here we present a brief overview of the method and how we integrate it in the computational pipeline we propose. Let us consider m snapshots representing the state of the system for a given time interval: $\{\boldsymbol{x}_i\}_{i=1}^m \in \mathbb{R}^n$. We seek a linear operator $\mathbf{A}$ to approximate the nonlinear dynamics of the state variable $\boldsymbol{x}$, that is $\boldsymbol{x}_{k+1} = \mathbf{A}\boldsymbol{x}_k$. In order to find the DMD decomposition

we only need to approximate the eigenpairs of the operator $\mathbf{A}$, without explicitly compute it. We proceed by dividing the snapshots in two matrices $\mathbf{X}$ and $\mathbf{Y}$ as in the following:

$$\mathbf{X} = \begin{bmatrix} x_1^1 & x_2^1 & \cdots & x_{m-1}^1 \\ x_1^2 & x_2^2 & \cdots & x_{m-1}^2 \\ \vdots & \vdots & \ddots & \vdots \\ x_1^n & x_2^n & \cdots & x_{m-1}^n \end{bmatrix}, \qquad \mathbf{Y} = \begin{bmatrix} x_2^1 & x_3^1 & \cdots & x_m^1 \\ x_2^2 & x_3^2 & \cdots & x_m^2 \\ \vdots & \vdots & \ddots & \vdots \\ x_2^n & x_3^n & \cdots & x_m^n \end{bmatrix}.$$

With this representation we seek $\mathbf{A}$ such that $\mathbf{Y} \approx \mathbf{A}\mathbf{X}$. Using the Moore-Penrose pseudo-inverse operator, denoted by †, we express the best-fit matrix as $\mathbf{A} = \mathbf{Y}\mathbf{X}^\dagger$. We can compute the POD modes of the matrix $\mathbf{X}$ and project the data onto the subspace defined by them. We use the truncated singular value decomposition obtaining $\mathbf{X} \approx \mathbf{U}_r\mathbf{\Sigma}_r\mathbf{V}_r^*$, where the unitary matrix $\mathbf{U}_r$ contains the first r modes. With these modes we can compute the reduced operator $\tilde{\mathbf{A}} \in \mathbb{C}^{r\times r}$ as $\tilde{\mathbf{A}} = \mathbf{U}_r^*\mathbf{A}\mathbf{U}_r = \mathbf{U}_r^*\mathbf{Y}\mathbf{X}^\dagger\mathbf{U}_r = \mathbf{U}_r^*\mathbf{Y}\mathbf{V}_r\mathbf{\Sigma}_r^{-1}\mathbf{U}_r^*\mathbf{U}_r = \mathbf{U}_r^*\mathbf{Y}\mathbf{V}_r\mathbf{\Sigma}_r^{-1}$, without the explicit computation of the full operator $\mathbf{A}$. The reduced operator describe the evolution of the low-rank approximated state $\tilde{\boldsymbol{x}}_k \in \mathbb{R}^r$ as $\tilde{\boldsymbol{x}}_{k+1} = \tilde{\mathbf{A}}\tilde{\boldsymbol{x}}_k$. We can then recover the high-dimensional state $\boldsymbol{x}_k$ using the POD modes already computed: $\boldsymbol{x}_k = \mathbf{U}_r\tilde{\boldsymbol{x}}_k$.

Using the eigendecomposition of the matrix $\tilde{\mathbf{A}}$, that is $\tilde{\mathbf{A}}\mathbf{W} = \mathbf{W}\mathbf{\Lambda}$, we are able to compute the eigenpairs of the full operator $\mathbf{A}$. In particular the eigenvalues in $\mathbf{\Lambda}$ correspond to the nonzero eigenvalues of $\mathbf{A}$, while the eigenvectors $\mathbf{\Phi}$ of $\mathbf{A}$ can be computed in two ways: by projecting the low-rank approximation $\mathbf{W}$ on the high-dimensional space $\mathbf{\Phi} = \mathbf{U}_r\mathbf{W}$, or by computing them exactly with $\mathbf{\Phi} = \mathbf{Y}\mathbf{V}_r\mathbf{\Sigma}_r^{-1}\mathbf{W}$.

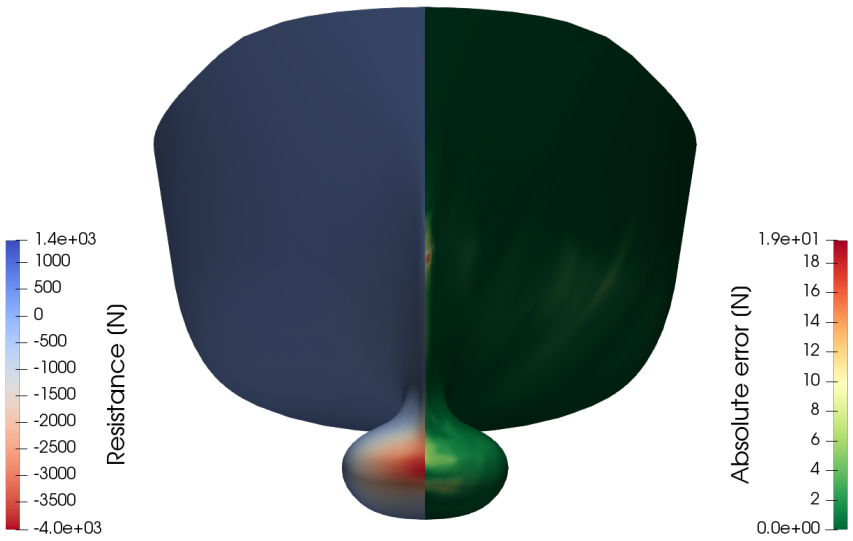

Figure 4: Example of total drag reconstructed using the DMD algorithm. On the left the reconstructed field, while on the right the absolute error with respect to the high-fidelity solution.

The actual implementation of the DMD algorithm we used and many different variants from

multiresolution DMD [18], to DMD with control [23], and higher order DMD [19], can be found in the open source Python package PyDMD [12].

In this work the DMD is used to accelerate the computation of the total drag resistance for a given deformed hull. It uses only few snapshots of the high-fidelity simulation, equispaced in time, to predict the evolution of the target output. In particular we are interested in the value of the total drag at regime. Figure 4 reports the forces field approximated using DMD and the absolute error with respect to the high-fidelity solution for a particular geometrical configuration.

4 How to reduce the parameter space dimension with active subspaces

The active subspaces (AS) property has been formalized by Constantine in [7, 8]. It is a property of a scalar function $f : \mathbb{R}^N \to \mathbb{R}$ and a probability density function $\rho : \mathbb{R}^N \to \mathbb{R}^+$, where N is the number of the input parameters. Taking linear combinations of the original parameters we can approximate f using these new parameters, thus reducing the parameter space dimension. The output of interest $f(\boldsymbol{\mu}_{\text{GEO}})$, in our case the total drag of the hull advancing in calm water, depends on the geometrical parameters introduced in Section 2, while ρ describe the uncertainty in the model inputs, i.e. how we sample the parameter space. For sake of clarity we will drop the pedix and from now on $f(\boldsymbol{\mu}) := f(\boldsymbol{\mu}_{\text{GEO}})$. The general idea is to rotate the input domain, after a proper rescale, in order to unveil a low dimensional parametrization of f, which means to find proper directions in the input space where f varies the most on average. We do so by checking the gradients of the output of interest with respect to the parameters.

To proper exploit the AS property we introduce some hypotheses: f has to be continuous and differentiable with square-integrable partial derivatives in the support of ρ. Then we introduce the uncentered covariance matrix $\mathbf{C}$ of the gradients of the target function, which is the matrix constructed with the average products of partial derivatives of the map f as follows

$$\mathbf{C} = \mathbb{E}\left[\nabla_{\boldsymbol{\mu}} f \, \nabla_{\boldsymbol{\mu}} f^T\right] = \int (\nabla_{\boldsymbol{\mu}} f)(\nabla_{\boldsymbol{\mu}} f)^T \rho \, d\boldsymbol{\mu}, \tag{3}$$

where with $\mathbb{E}$ we identify the expected value, and $\nabla_{\boldsymbol{\mu}} f = \nabla f(\boldsymbol{\mu}) = \left[\frac{\partial f}{\partial \mu_1}, \dots, \frac{\partial f}{\partial \mu_p}\right]^T$ is the column vector of partial derivatives of f. Since $\mathbf{C}$ is symmetric we can express it with its real eigenvalue decomposition $\mathbf{C} = \mathbf{W}\boldsymbol{\Lambda}\mathbf{W}^T$, where $\mathbf{W}$ is the eigenvectors matrix, and $\boldsymbol{\Lambda}$ the diagonal matrix with the eigenvalues in descending order. It can be proven that the eigenvalues express the amount of variance of the gradient along the corresponding eigenvector direction. This means that taking the first M most energetic eigenvalues and the corresponding eigenvectors, we can approximate the target function with a reduce number of input parameters. So the eigenpairs of $\mathbf{C}$ define the active subspaces of the pair (f, ρ). We proceed by partitioning $\mathbf{W}$ and $\boldsymbol{\Lambda}$ as follows

$$\boldsymbol{\Lambda} = \begin{bmatrix} \boldsymbol{\Lambda}_1 & \\ & \boldsymbol{\Lambda}_2 \end{bmatrix}, \qquad \mathbf{W} = \begin{bmatrix} \mathbf{W}_1 & \mathbf{W}_2 \end{bmatrix}, \tag{4}$$

where the pedix 1 means the first M eigenvalues and eigenvectors respectively. Now we can use $\mathbf{W}_1$ to project the original parameters to the active subspace, that is the span of the first M eigenvectors. This means to align the input parameter space to $\mathbf{W}_1$ and retain only the directions where f varies the most on average. We call active variable $\boldsymbol{\mu}_M$ the range of $\mathbf{W}_1^T$,

that is $\boldsymbol{\mu}_M = \mathbf{W}_1^T \boldsymbol{\mu} \in \mathbb{R}^M$. We can thus introduce a lower-dimension approximation $g : \mathbb{R}^M \to \mathbb{R}$ of the quantity of interest f, which is a function of $\boldsymbol{\mu}_M$ as follows

$$f(\boldsymbol{\mu}) \approx g(\mathbf{W}_1^T \boldsymbol{\mu}) = g(\boldsymbol{\mu}_M). \tag{5}$$

Active subspaces have been proven useful in naval applications in [38, 36, 10], but also coupled with POD-Galerkin model order reduction [35]. A gradient-free algorithm for the discovery of active subspaces has been proposed in [6], while an AS variant using average gradients in [20].

We are going to find the active subspace for the total drag resistance of the deformed hulls obtained by the FFD method and the application of the DMD algorithm. Then we are going to exploit this active subspace to perform a better sampling of the parameter space and thus enhancing the construction of the reduced order model.

5 Proper orthogonal decomposition with interpolation

Reduced order modeling (ROM) is a popular technique to reduce the computational cost of numerical simulations. Among all the available methods to achieve this reduction, we focus in this contribution to the reduced basis method using the proper orthogonal decomposition (POD) algorithm for the basis identification. This method allows to reduce the number of degrees of freedom of a parametric system by collecting the *snapshots* — the full order system outputs — for several different configurations and combining them in an efficient way for a real-time approximation of new solutions (for any new configuration). In the POD reduction framework, we can discern two main techniques: POD-Galerkin, which requires all the details of the full order system to generate a consistent low-dimensional representation of the physical problem, and POD with interpolation (PODI), which instead requires only the snapshots. Due to these requirements, the PODI method is particularly suited for industrial problem, since it is able to been coupled to all the numerical solvers, even commercial ones. In this contribution, we adopt PODI method. For more information about POD-Galerkin, we suggest [34, 33, 16, 15], while for other examples of PODI applications we recommend [14, 11, 28].

To calculate the POD modes we use the singular value decomposition (SVD) applied to the snapshots matrix $\mathbf{X}$ such that $\mathbf{X} = \mathbf{U}\boldsymbol{\Sigma}\mathbf{V}^*$. The columns of the unitary matrix $\mathbf{U}$ are the POD modes end the corresponding singular values, the elements in the diagonal matrix $\boldsymbol{\Sigma}$ in decresing order, indicate the energy associated to each mode. Hence it is possible to select the first modes — the most energetic — to span the reduced space and project onto it the high-fidelity snapshots. In matricial form, we have:

$$\mathbf{X}^{\text{POD}} = \mathbf{U}_N^T \mathbf{X}, \tag{6}$$

where $\mathbf{U}_N$ is the matrix containing the first N modes, and $\mathbf{X}^{\text{POD}}$ is the matrix whose columns $\mathbf{x}_i^{\text{POD}}$ are the reduced snapshots. We note that $\mathbf{x}_i^{\text{POD}} \in V^N$ and $\mathbf{x}_i \in V^{\mathcal{N}}$ where $\mathcal{N}$ refers to the number of degrees of freedom of the full-order system. Finally, due to the reduced dimension, we are able to interpolate the reduced snapshots in order to approximate the solution manifold. The new interpolated reduced snapshots are then mapped back to the high-dimensional space for a real-time evaluation of the solution. To perform the non-intrusive model order reduction, we use the open source package EZyRB [11].

6 Numerical results

Here we are going to present the results of the complete numerical pipeline applied to the DTMB 5415 hull. Moreover we demonstrate the improvements obtained using the proposed pipeline, called POD+AS, with respect to the POD approach on the full parameter space.

After generating $N_{\text{POD}} = 100$ deformed hulls, we perform the high-fidelity simulations accelerated via the DMD algorithm. We construct the snapshots matrix and compute the POD modes and the corresponding eigenvalues for the construction of the reduced output space. We compare this approach with the one proposed in this work that exploits a preprocessing step with the finding of the active subpace for the total drag resistance. With the N_{POD} input/output couples, we individuate an eigenvector $\mathbf{W}_1$ (compare Section 4) describing an active subspace of dimension 1, and we sample the full space only along the active direction described by this vector. After this second sampling we collect a new set of high-fidelity simulations formed by $N_{\text{POD+AS}} = 80$ snapshots. For this new snapshots matrix we compute again the POD modes and eigenvalues, and we compare the two approaches looking at the POD singular values decay. A faster decay means a better approximation of the output fields for a fixed number of modes. In Figure 5 the blue line shows the singular values σ_i divided by the first and greatest singular value $\sigma_{\max}$ for the sampling of the full parameter space; with the dashed red line the POD singular values decay for the POD+AS approach. A faster decay is observed, especially for the first few modes. This translates in an enhanced reduced order model, which exhibits a better approximation of the solutions manifold, with respect to the classical approach.

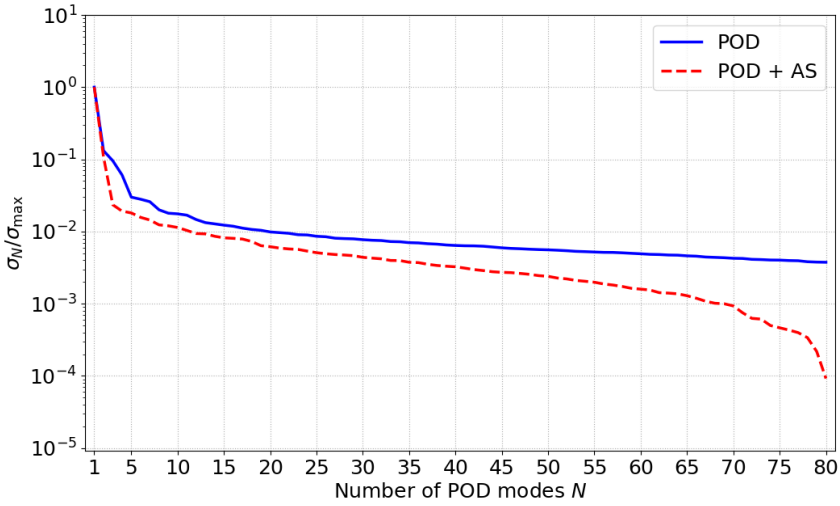

Figure 5: POD singular values decay as a function of the number of modes. The blue line corresponds to the original sampling, while the red dotted line, called POD+AS approach, corresponds to the sampling along the active direction.

Since we are relying on multidimensional interpolation to reconstruct the solutions at untried

parameters, having a new reduced parameter space improves the creation of such interpolator. In the POD+AS approach we have to interpolate a univariate function in N-dimension, where N is the number of POD modes we retain. In the POD approach on the full parameter space instead, we have the same number of modes to fit but a multivariate function depending on 5 input parameters, resulting in a difficult interpolation.

7 Conclusions and perspectives

In this work we presented a nonintrusive numerical pipeline for shape optimization of the bulbous bow of a benchmark hull. It comprises automatic geometrical parametrization and morphing through FFD, estimation of the total drag resistance via DMD using only few snapshots of the time-dependent high fidelity simulations, the reduction of the parameter space exploiting the AS property, and the construction of a surrogate model with PODI for the real-time evaluation of the many-query problem solved by an optimization algorithm. We proved that the reduction of the parameter space can further enhance the reduced order model creation. Moreover all this parts of the pipeline can be used and integrated separately into an existing computational workflow resulting in a great interest for industrial applications.

Acknowledgements

This work was partially performed in the context of the project SOPHYA - "Seakeeping Of Planing Hull YAchts" supported by Regione FVG, POR-FESR 2014-2020, Piano Operativo Regionale Fondo Europeo per lo Sviluppo Regionale, and partially supported by European Union Funding for Research and Innovation — Horizon 2020 Program — in the framework of European Research Council Executive Agency: H2020 ERC CoG 2015 AROMA-CFD project 681447 "Advanced Reduced Order Methods with Applications in Computational Fluid Dynamics" P.I. Gianluigi Rozza.

REFERENCES

[1] PyGeM: Python Geometrical Morphing. Available at: `https://github.com/mathLab/PyGeM`.

[2] F. Ballarin, A. D'Amario, S. Perotto, and G. Rozza. A POD-selective inverse distance weighting method for fast parametrized shape morphing. *International Journal for Numerical Methods in Engineering*, 117(8):860–884, 2018.

[3] D. Bistrian and I. Navon. Efficiency of randomised dynamic mode decomposition for reduced order modelling. *International Journal of Computational Fluid Dynamics*, 32(2-3):88–103, 2018.

[4] D. A. Bistrian and I. M. Navon. Randomized dynamic mode decomposition for nonintrusive reduced order modelling. *International Journal for Numerical Methods in Engineering*, 112(1):3–25, 2017.

[5] M. D. Buhmann. *Radial basis functions: theory and implementations*, volume 12. Cambridge university press, 2003.

[6] K. D. Coleman, A. Lewis, R. C. Smith, B. Williams, M. Morris, and B. Khuwaileh. Gradient-free construction of active subspaces for dimension reduction in complex models with applications to neutronics. *SIAM/ASA Journal on Uncertainty Quantification*, 7(1):117–142, 2019.

[7] P. G. Constantine. *Active subspaces: Emerging ideas for dimension reduction in parameter studies*, volume 2. SIAM, 2015.

[8] P. G. Constantine, E. Dow, and Q. Wang. Active subspace methods in theory and practice: applications to kriging surfaces. *SIAM Journal on Scientific Computing*, 36(4):A1500–A1524, 2014.

[9] N. Demo, M. Tezzele, G. Gustin, G. Lavini, and G. Rozza. Shape optimization by means of proper orthogonal decomposition and dynamic mode decomposition. In *Technology and Science for the Ships of the Future: Proceedings of NAV 2018: 19th International Conference on Ship & Maritime Research*, pages 212–219. IOS Press, 2018.

[10] N. Demo, M. Tezzele, A. Mola, and G. Rozza. An efficient shape parametrisation by free-form deformation enhanced by active subspace for hull hydrodynamic ship design problems in open source environment. In *The 28th International Ocean and Polar Engineering Conference*, 2018.

[11] N. Demo, M. Tezzele, and G. Rozza. EZyRB: Easy Reduced Basis method. *The Journal of Open Source Software*, 3(24):661, 2018.

[12] N. Demo, M. Tezzele, and G. Rozza. PyDMD: Python Dynamic Mode Decomposition. *The Journal of Open Source Software*, 3(22):530, 2018.

[13] D. Forti and G. Rozza. Efficient geometrical parametrisation techniques of interfaces for reduced-order modelling: application to fluid–structure interaction coupling problems. *International Journal of Computational Fluid Dynamics*, 28(3-4):158–169, 2014.

[14] F. Garotta, N. Demo, M. Tezzele, M. Carraturo, A. Reali, and G. Rozza. Reduced Order Isogeometric Analysis Approach for PDEs in Parametrized Domains. *Submitted, QUIET special volume*, 2018.

[15] S. Georgaka, G. Stabile, G. Rozza, and M. J. Bluck. Parametric pod-galerkin model order reduction for unsteady-state heat transfer problems. *arXiv preprint arXiv:1808.05175*, 2018.

[16] E. N. Karatzas, F. Ballarin, and G. Rozza. Projection-based reduced order models for a cut finite element method in parametrized domains. *arXiv preprint arXiv:1901.03846*, 2019.

[17] J. N. Kutz, S. L. Brunton, B. W. Brunton, and J. L. Proctor. *Dynamic mode decomposition: data-driven modeling of complex systems*, volume 149. SIAM, 2016.

[18] J. N. Kutz, X. Fu, and S. L. Brunton. Multiresolution dynamic mode decomposition. *SIAM Journal on Applied Dynamical Systems*, 15(2):713–735, 2016.

[19] S. Le Clainche and J. M. Vega. Higher order dynamic mode decomposition. *SIAM Journal on Applied Dynamical Systems*, 16(2):882–925, 2017.

[20] M. R. Lee. Modified active subspaces using the average of gradients. *SIAM/ASA Journal on Uncertainty Quantification*, 7(1):53–66, 2019.

[21] A. Manzoni, A. Quarteroni, and G. Rozza. Model reduction techniques for fast blood flow simulation in parametrized geometries. *International journal for numerical methods in biomedical engineering*, 28(6-7):604–625, 2012.

[22] A. Morris, C. Allen, and T. Rendall. CFD-based optimization of aerofoils using radial basis functions for domain element parameterization and mesh deformation. *International Journal for Numerical Methods in Fluids*, 58(8):827–860, 2008.

[23] J. L. Proctor, S. L. Brunton, and J. N. Kutz. Dynamic mode decomposition with control. *SIAM Journal on Applied Dynamical Systems*, 15(1):142–161, 2016.

[24] G. Rozza, M. W. Hess, G. Stabile, M. Tezzele, and F. Ballarin. Preliminaries and warming-up: Basic ideas and tools. In P. Benner, S. Grivet-Talocia, A. Quarteroni, G. Rozza, W. H. A. Schilders, and L. M. Silveira, editors, *Handbook on Model Order Reduction*, volume 1, chapter 1. De Gruyter, 2019.

[25] G. Rozza, A. Koshakji, and A. Quarteroni. Free Form Deformation techniques applied to 3D shape optimization problems. *Communications in Applied and Industrial Mathematics*, 4(0):1–26, 2013.

[26] G. Rozza, M. H. Malik, N. Demo, M. Tezzele, M. Girfoglio, G. Stabile, and A. Mola. Advances in Reduced Order Methods for Parametric Industrial Problems in Computational Fluid Dynamics. Glasgow, UK, 2018. ECCOMAS Proceedings.

[27] F. Salmoiraghi, F. Ballarin, G. Corsi, A. Mola, M. Tezzele, and G. Rozza. Advances in geometrical parametrization and reduced order models and methods for computational fluid dynamics problems in applied sciences and engineering: Overview and perspectives. *ECCOMAS Congress 2016 - Proceedings of the 7th European Congress on Computational Methods in Applied Sciences and Engineering*, 1:1013–1031, 2016.

[28] F. Salmoiraghi, A. Scardigli, H. Telib, and G. Rozza. Free-form deformation, mesh morphing and reduced-order methods: enablers for efficient aerodynamic shape optimisation. *International Journal of Computational Fluid Dynamics*, 0(0):1–15, 2018.

[29] P. J. Schmid. Dynamic mode decomposition of numerical and experimental data. *Journal of fluid mechanics*, 656:5–28, 2010.

[30] P. J. Schmid, L. Li, M. P. Juniper, and O. Pust. Applications of the dynamic mode decomposition. *Theoretical and Computational Fluid Dynamics*, 25(1-4):249–259, 2011.

[31] T. Sederberg and S. Parry. Free-Form Deformation of solid geometric models. In *Proceedings of SIGGRAPH - Special Interest Group on GRAPHics and Interactive Techniques*, pages 151–159. SIGGRAPH, 1986.

[32] D. Shepard. A two-dimensional interpolation function for irregularly-spaced data. In *Proceedings-1968 ACM National Conference*, pages 517–524. ACM, 1968.

[33] G. Stabile, S. N. Hijazi, S. Lorenzi, A. Mola, and G. Rozza. Pod-galerkin reduced order methods for cfd using finite volume discretisation: Vortex shedding around a circular cylinder. *Communication in Applied Industrial Mathematics*, 8(1):210–236, dec 2017.

[34] G. Stabile and G. Rozza. Finite volume pod-galerkin stabilised reduced order methods for the parametrised incompressible navier–stokes equations. *Computers & Fluids*, 173:273–284, 2018.

[35] M. Tezzele, F. Ballarin, and G. Rozza. Combined parameter and model reduction of cardiovascular problems by means of active subspaces and POD-Galerkin methods. In D. Boffi, L. F. Pavarino, G. Rozza, S. Scacchi, and C. Vergara, editors, *Mathematical and Numerical Modeling of the Cardiovascular System and Applications*, pages 185–207. Springer International Publishing, 2018.

[36] M. Tezzele, N. Demo, M. Gadalla, A. Mola, and G. Rozza. Model order reduction by means of active subspaces and dynamic mode decomposition for parametric hull shape design hydrodynamics. In *Technology and Science for the Ships of the Future: Proceedings of NAV 2018: 19th International Conference on Ship & Maritime Research*, pages 569–576. IOS Press, 2018.

[37] M. Tezzele, N. Demo, A. Mola, and G. Rozza. An integrated data-driven computational pipeline with model order reduction for industrial and applied mathematics. *Submitted, Special Volume ECMI*, 2018.

[38] M. Tezzele, F. Salmoiraghi, A. Mola, and G. Rozza. Dimension reduction in heterogeneous parametric spaces with application to naval engineering shape design problems. *Advanced Modeling and Simulation in Engineering Sciences*, 5(1):25, Sep 2018.